

Supporting Information:

Far-field Wavefront Control of Nonlinear Luminescence in Disordered Gold Metasurfaces

Gauthier Roubaud,[†] Pierre Bondareff,[†] Giorgio Volpe,^{‡,¶} Sylvain Gigan,[‡]

Sébastien Bidault,^{*,†} and Samuel Grésillon^{*,†}

[†]*Institut Langevin, ESPCI Paris, PSL University, CNRS, Sorbonne Université, 1 rue Jussieu, F-75005 Paris, France*

[‡]*Laboratoire Kastler Brossel, Sorbonne Université, École Normale Supérieure–PSL University, CNRS, Collège de France, 24 rue Lhomond, 75005 Paris, France*

[¶]*Current address: Department of Chemistry, University College London, 20 Gordon Street, London, WC1H 0AJ, UK*

E-mail: sebastien.bidault@espci.fr; samuel.gresillon@espci.fr

Experimental procedures

Disordered gold metasurfaces are produced by electron-beam deposition of a few nanometers thick layer of gold on a freshly cleaned glass coverslip in a vacuum chamber (Oerlikon). The filling fraction of gold in the surface is defined as $ff = s_m/(s_m + s_g)$, where s_m and s_g are the surfaces covered by gold and glass, respectively. Electrical percolation is observed when the filling fraction reaches a threshold value of the order of 0.65.^{S1,S2}

Collimated light from a femtosecond pulsed laser at 790 nm (Mira 900, Coherent, 200 fs, 80 MHz) is reflected by a spatial light modulator (SLM, LCOS 10468-02, Hamamatsu, 792×600 pixels, 20 μm pixel size) before being conjugated with the image plane of an inverted microscope using a 1.4 NA (60×) objective (Eclipse Ti, Nikon). The optical setup is also designed to focus the incoming laser on the Fourier plane of the microscope objective so that the excitation is collimated on the sample with an excitation intensity of 1 kW/cm² (it should not exceed 10 MW/cm² to avoid damaging the gold surface). Nonlinear photoluminescence emitted by the disordered gold surface is collected by the same objective before being spectrally filtered between 450 nm and 650 nm, and imaged on a sCMOS camera (Edge 5.5, PCO, 2560×2160 pixels, 6.5 μm pixel size). Considering the magnification in excitation and detection, the pixels of the SLM and of the camera correspond to 180 nm and 100 nm squares on the sample surface. For the SLM, 4 pixels are binned to provide macropixels that are closer in size to the diffraction limit in excitation. The microscope objective is mounted on a piezoelectric holder (P-721 PIFOC, PI) in order to perform an autofocus of the NPL image at the beginning of the optimization algorithm. This allows an automatic implementation of up to 10 procedures consecutively. Finally, the sample is mounted on a 3D piezoelectric stage (P-517.3CD, PI), allowing the measurement of the nonlinear luminescence signal as a function of the position of the sample (see Fig. 4-c of the main text).

The imaging diffraction limit for the NPL intensity is estimated using isolated 80 nm gold particles (British Biocell) spin-coated on a glass coverslip (see Fig. S1). Complementary two-photon fluorescence (TPF) experiments are performed with the same optical setup but

using a $1\text{ }\mu\text{m}$ thick layer of polyvinyl alcohol doped with fluorescein (1% weight-to-weight) and spin-coated on a freshly cleaned glass coverslip. Apart from the estimation of the non-linear intensity dependence of the NPL and TPF signals, all measurements are performed with the same excitation intensity.

The iterative optimization algorithm^{S3,S4} starts with a fully random phase pattern on the entire SLM surface. For each experiment, the wavefront-shaped area corresponds to a square of several tens of pixels in which the phases will be tuned. As explained in the main text, half of the pixels of the wavefront-shaped area are randomly selected for each iteration. Optimization of the NPL signal in the center of the wavefront-shaped area is performed by tuning the phase of these pixels over 4 values: 0 , $\pi/2$, π and $3\pi/2$. A fifth measurement with a phase of 2π is used to verify the stability of the measurement by comparing the corresponding NPL image with the one observed with a 0 phase. The optimization targets an increase of the highest NPL intensity from one of the 9 pixels in the center of the wavefront-shaped area. The process is performed over 130 iterations, corresponding to a duration of 15 min. In more than 75% of the measurements, the highest NPL intensity is obtained before iteration 100, indicating that this duration is sufficient to provide the highest possible signal when only considering 4 phases. Furthermore, the mechanical stability of the optical setup does not allow longer experiments: indeed, Fig. 4-c of the main text shows how optimized NPL intensities typically decrease by 80% if the sample is displaced by a few hundred nanometers. Furthermore, weak defocusing of the luminescence image during the optimization also hinders the ability of the iterative algorithm to optimize the NPL signal. To ensure that this issue does not occur in our measurements, we perform a second image of the NPL intensity with the best wavefront selected by the algorithm at the end of the optimization process: if the second image is defocused with respect to the one measured during the optimization and/or if the spatial correlation between the two images is below 0.6, then this optimization procedure is not considered. In practice, less than 10% of the measurements are removed from the final statistical analysis.

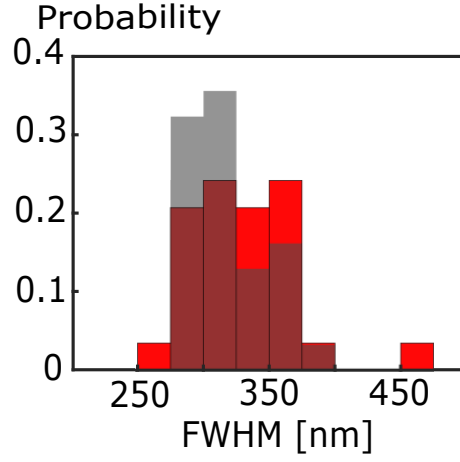


Figure S1: Distributions of full-width at half maxima (FWHM) for nonlinear photoluminescence (NPL) images of single 80 nm gold particles (grey data) and of optimized areas after the random iterative algorithm (red data). These measurements demonstrate that the optimized NPL intensity, after wavefront shaping, originates from a diffraction-limited area.

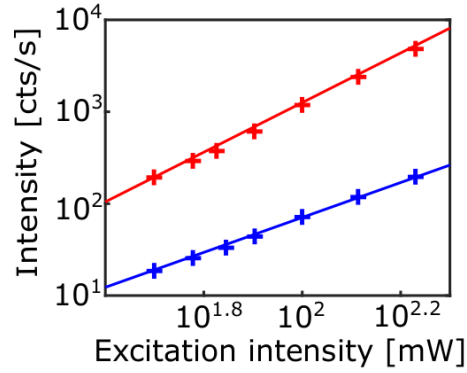


Figure S2: Averaged NPL (gold metasurface at the percolation threshold, red data points) and TPF (fluorescein-doped film, blue data points) intensities, averaged over 10^4 pixels around the center of the wavefront-shaped area, as a function of the excitation intensity. The solid lines are linear fits: the slopes are equal to 2 for the TPL signal and 2.8 for the NPL intensity, respectively.

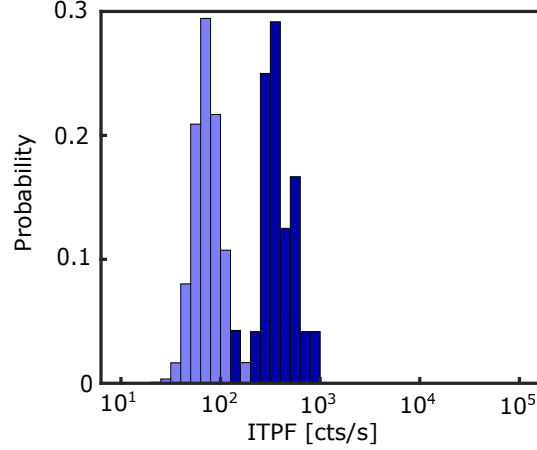


Figure S3: (Distributions of TPF intensities measured on a homogeneous fluorescent film before and after 28 iterative optimizations. The initial TPF intensities are estimated over 10^4 pixels around the optimized position (center of the wavefront-shaped area). The final TPF intensities are estimated as the largest value in the 9 pixels around the optimized position. The means of these log-normal distributions indicate an average enhancement of 6.

References

- (S1) Gadenne, P.; Rivoal, J. C. In *Optical Properties of Nanostructured Random Media*; Shalaev, V. M., Ed.; Springer Berlin Heidelberg, 2002; p 187–215.
- (S2) Seal, K.; Sarychev, A. K.; Noh, H.; Genov, D. A.; Yamilov, A.; Shalaev, V. M.; Ying, Z. C.; Cao, H. Near-Field Intensity Correlations in Semicontinuous Metal-Dielectric Films. *Phys. Rev. Lett.* **2005**, *94*, 226101.
- (S3) Vellekoop, I. M.; Mosk, A. P. Phase control algorithms for focusing light through turbid media. *Opt. Commun.* **2008**, *281*, 3071–3080.
- (S4) Conkey, D. B.; Brown, A. N.; Caravaca-Aguirre, A. M.; Piestun, R. Genetic algorithm optimization for focusing through turbid media in noisy environments. *Opt. Express* **2012**, *20*, 4840–4849.